

Comparative CFD Analysis of Heat Transfer and Melting Characteristics of the PCM in Enclosures with Different Fin Configurations



Arun Uniyal and Yogesh K. Prajapati

1 Introduction

In the current scenario, demand of uninterrupted energy supply is continuously increasing. It is due to the fact that day to day activities and life style of the mankind are mainly governed by energy consuming appliances. It is well known that thermal energy in one of the most usable forms of energies required in various applications. Over the period of time several techniques have been developed to store the thermal energy that holds the potential to fulfil the continuous energy supply. Available thermal energy received through the solar radiation is available in abundant amount, if it could be stored judiciously during the sunshine hours this stored energy can provide the heat according to demand. Phase Change Materials (PCM) have been recognized as the materials that can store and release the energy by changing its phase. Such materials have gained more attention in recent times due to their large latent heat capacity and economical aspects. PCMs have wide range of applications, that is, electronic industry, textile industry, battery thermal management system, solar energy storage [1–3].

2 Literature Review and Objective

It is worth mentioning that usually PCM have low-thermal conductivity. Hence, in the literature, consistent efforts have been made towards increasing the thermal conductivity of the PCM [9, 11].

A. Uniyal (✉)

Department of Mechanical Engineering, NIT Uttarakhand, Srinagar, Garhwal 246174, India
e-mail: arun.uniyal1990@gmail.com

Y. K. Prajapati

Department of Mechanical Engineering, BIT Sindri, Dhanbad, Jharkhand 828123, India

Besides, insertion of fins is one of the most effective techniques for enhancing the thermal conductivity inside the PCM enclosure. Several researchers have made significant contribution in this field. Ji et al. [4] have proposed the inclined fins in the rectangular domain of the PCM. They observed significant improvement in the melting rate if the fin was placed inclined at an angle of -15° consequently, 62.7% time was saved in complete melting of the PCM. Chen et al. [5] have used double triangular fins in a rectangular section using nanocomposite. Results revealed that volume fraction of 1% of nanoparticle exhibits the best performance and saved 184 s time compared with pure PCM. Samakoush et al. [6] examined the combination of triangular and rectangular fins. Results show that in a case with six proposed fins witness higher melting rate and reduces the melting period by 57.56% as compared to no fin configurations.

Additionally, literature survey confirms that availability of fins in the PCM domain certainly helps in enhancing the heat transfer characteristic of the PCM. Henceforth, most of the researchers have proposed different types of fin configurations to further improve the performance. In the present work, comparative study has been performed to compare the performance of different fin configuration while keeping the equal fins heat transfer area in all the cases. Please note that four different fin configurations, that is, single rectangular, double rectangular, triple rectangular and triangular fins are used in the square domain to understand the melting characteristics, enhancement ratio and impact of natural convective currents on melting characteristics of PCM.

3 Geometrical Description

Different fin configurations of the rectangular and triangular fins inside the square domain (size = 20 mm) of the PCM have been presented in a Fig. 1. Five cases have been considered where fins surface area in each case is constant (30 mm^2). In order to maintain the equal fin surface area, fin length and width are varied in the domain. Except 4th case, length of the fin is taken as 15 mm and whereas, fin thickness is kept 1 and 2 mm. In the case 5, base of the triangular fins are 2 mm. Paraffin wax is taken as phase change material whose property has been given in Table 1. PCM is filled inside the square domain of dimension 20 mm. A constant temperature source (350 K) is applied on left side edge of the domain and rest sides of the domain are adiabatic in nature.

3.1 Numerical Methodology and Governing Equation

Two-dimensional (2D) numerical simulation has been conducted using ANSYS Fluent. Phase change process of the PCM has been modelled using enthalpy porosity

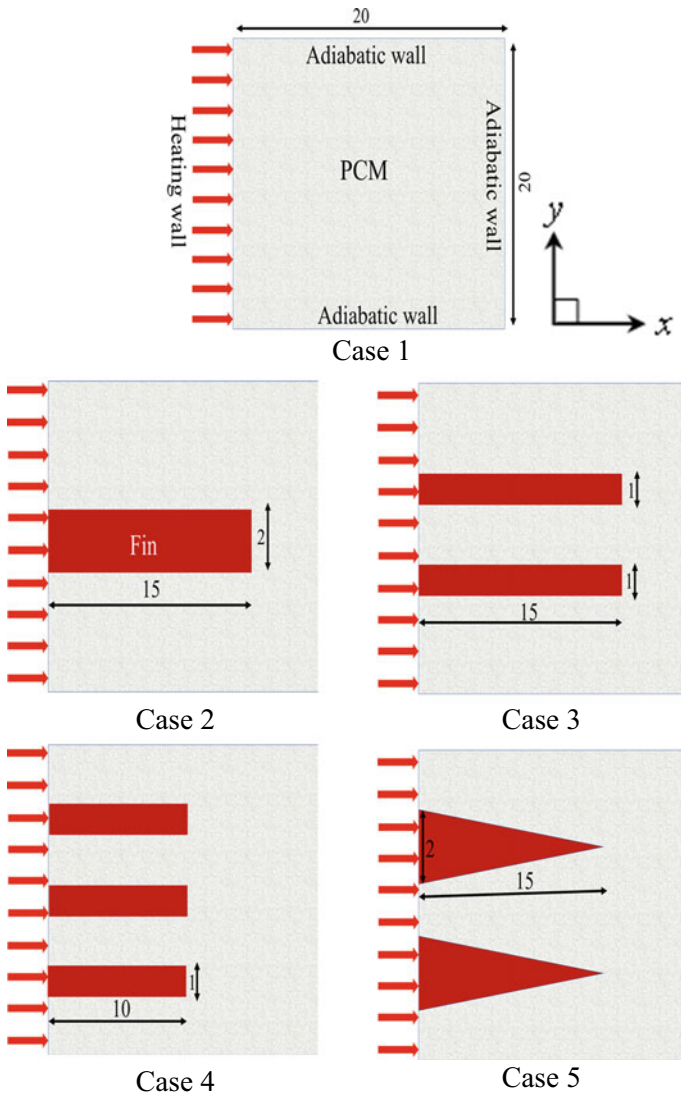


Fig. 1 Schematic diagram of different cases in square PCM domain (all dimensions are in mm)

method [8]. Following assumptions were considered during in the numerical simulation: (a) Liquid PCM is assumed as incompressible and Newtonian fluid. (b) Thermophysical properties of the PCM remains constant. (c) The volume of the PCM remain constant before and after the melting process (d) No heat loss occurs from the square domain.

It is understood that in the melting process of the PCM, natural convection will play significant role hence, it has been considered by introducing the Boussinesq

Table 1 Thermophysical properties of paraffin wax [10]

Parameter	Value
Thermal conductivity [W/m-K]	0.21
Heat of fusion [kJ/kg]	189
Density [kg/m ³]	795/920
Specific heat [kJ/kg-K]	2/2.15
Dynamic viscosity of liquid paraffin [kg/m-s]	0.023
Thermal expansion coefficient [1/K]	0.0003085

equation. Following governing equations have been used in the present numerical model.

$$\rho = \frac{\rho}{[\beta(T - T_{liquids}) + 1]} \quad (1)$$

The continuity may be written as:

$$\frac{\partial}{\partial t} \rho + \nabla \cdot (\rho \vec{V}) = 0 \quad (2)$$

Equation below represents the momentum equation:

$$\frac{\partial}{\partial t} (\rho V) + \nabla \cdot (\rho \vec{V} \vec{V}) = (\mu \nabla^2 \vec{V} - \nabla \rho + \rho \vec{g}) + \vec{S} \quad (3)$$

In the above equation, \vec{S} denotes the source term. This term has been added to consider the natural convection in the melting process.

$$\vec{S} = -A_{mushy} \left[\frac{(1 - \lambda)^2}{\lambda^3 + e} \right] \times \vec{V} \quad (4)$$

where A_{mushy} is the mushy zone constant which helps in measuring the damping behaviour. The value of A_{mushy} varies from 10^4 to 10^7 .

Following energy equation is solved:

$$\frac{\partial}{\partial t} (\rho H) + \nabla \cdot (\rho \vec{V} H) = \nabla \cdot (k \nabla T) \quad (5)$$

The total enthalpy contains both sensible as well as latent heat:

$$h_{total} = h_{sen} + h_{lat} \quad (6)$$

Sensible and latent heat have been calculated from the following equations:

$$h_{sen} = h_{ref} + c_p \int_{T_{ref}}^T dT \quad (7)$$

$$h_{lat} = \sum_{i=1}^n \lambda_i h_{sf} \quad (8)$$

where λ is the liquid fraction, its value varies from 0 to 1 for each computational cell and it is considered as mushy zone when λ varies between 0 and 1. $\lambda = 0$ indicates that cell is in solid state while $\lambda = 1$ indicates that cell consists of liquid state.

3.2 Initial and Boundary Conditions

In the present study numerical model, a constant temperature source of 350 K has been applied on the left side of square domain. PCM is kept at initial temperature of 303 K. Gravity force has been applied along Y-axis. As mentioned in the above section, ANSYS Fluent is used for the simulation, SIMPLE scheme and first-order implicit method are used for the pressure velocity coupling and transient formulation, respectively. Pressure correction equation has been solved by PRESTO scheme. Momentum and energy equations are discretized by second-order upwind scheme. Convergence criteria of are set at 10^{-4} , 10^{-4} , 10^{-6} are set respectively for continuity, momentum and energy equations.

3.3 Grid Independency Test and Model Validation

In order to perform the grid independency test four distinct element sizes 0.2 mm, 0.15 mm, 0.1 mm, 0.08 mm have been taken. Figure 2a describes the variation of liquid fraction with respect to time for different size of elements. It can be seen that with varying element size, liquid fraction is almost similar and maximum variation in results is found to be 1.48%. Hence, grid size of 0.1 mm is taken for all the simulations.

The current numerical model has been validated with the experimental work of Kamkari et al. [7]. Identical geometry of Kamkari et al. has been generated and Lauric acid is considered as the PCM. Besides, similar initial and boundary conditions have been used. Results have been compared in Fig. 2b, it may be seen that present model closely predicts the liquid fraction with Kamkari et al. with maximum deviation of 7–10%.

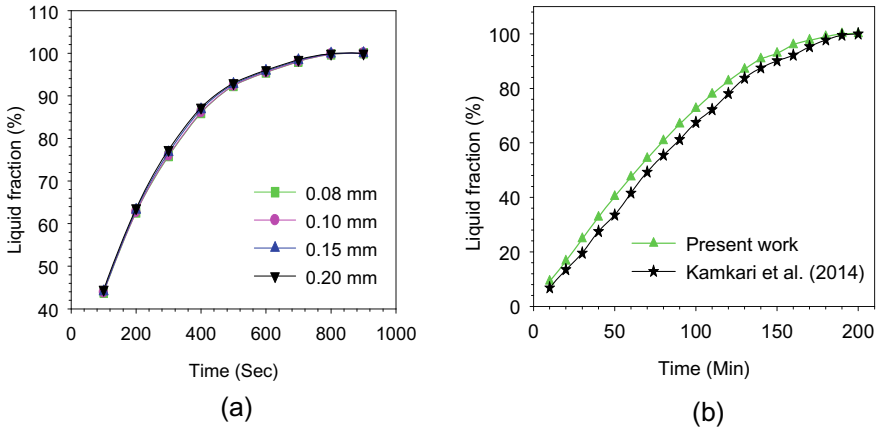


Fig. 2 a Grid independency test. b Validation of the present work with Kamkari et al. [7]

4 Results and Discussion

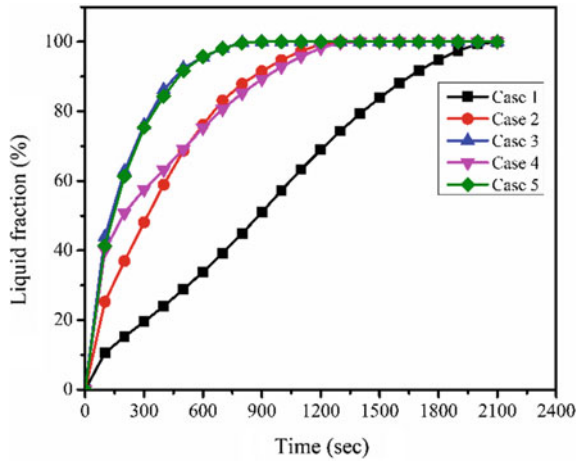
The comparative results of all the five configurations have been discussed to comprehend the heat transfer rate, melting characteristics of the PCM and enhancement ratio. Besides, different contour plots are drawn to visualize the stream lines patterns and phase change process of the PCM in the domain.

4.1 Melting Characteristics of the PCM

In order to understand the charging (melting) characteristics of the phase change material, it is necessary to predict the energy storage rate. In the literature, several attempts have been made to expedite the melting rate which results in decrease in energy storing time. Figure 3 illustrates the liquid fraction of the PCM with respect to time for all the five cases at the fixed wall temperature of 350 K. Figure 3 shows that owing to different melting rates, slopes of the curves are dissimilar for different cases. First configuration without any fin deliberates the least slope as compared to other cases. It indicates that melting rate of the PCM is slowest in this domain. Unavailability of the fins lowers the heat transfer from the heated wall to the remaining portion of the domain. Therefore, melting process is delayed consequently, it takes 2073 sec to melt the complete PCM.

However, slopes of the other curves representing finned configuration are considerably different. It may be seen that curves are quite steeper at the beginning and with passage of time it flattens which indicates that melting process is rapid at the beginning, however, slow melting occurs at the end. It is understood that heat is being propagated from the left to the right of the square enclosure. PCM is first melted at

Fig. 3 Variation of liquid fraction with respect to time for each case



the left side of the domain and gradually solid–liquid interface moves away from heat wall. Inclusion of fins expedites the heat dissipation from heated wall to remaining portion of the domain which leads to faster melting. Since the fin length is restricted up to 15 mm, the portion of the enclosure located far away from the fins receives less heat hence; slow melting of the PCM was experienced.

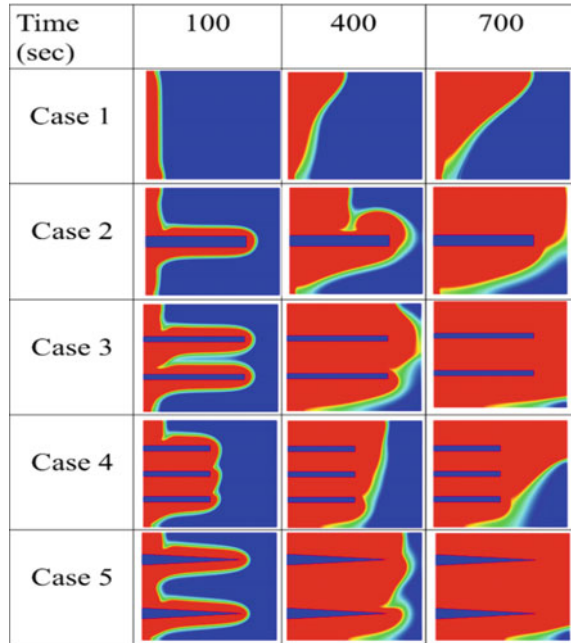
It has been reported that initially (up to 100 sec), cases 3, 4 and 5 have nearly same melting rate which is $\approx 30\%$ higher than case 1. Whereas, melting rate of the PCM in 2nd domain is only $\approx 15\%$ higher as compared to case 1. Since 2nd domain holds only single fin which is mainly concentrated to the middle of the PCM domain.

Further, it may be noted that case 3 and 5 show nearly similar trends and both of them have been melted completely (100% melting) within 820 seconds which is 60.44% higher than the case 1. Among the finned configurations, least performance is given by case 4. This is mainly due to the presence of shorter fins which restricts the heat transfer up to the middle portion of the domain, beyond it, slower heat transfer occurs through PCM.

In order to have deep insights of the melting phenomenon of the PCM, liquid fraction contours are shown in Fig. 4 at different time intervals. Please note that blue and red colours represent solid and liquid phases of the PCM, respectively. Uniform thickness of the melted PCM has been observed in case 1 within 100 secs. Over the period of time, amount of melted PCM increases in the entire domain. Additionally, it can be seen that the thickness of melted PCM considerably reduces from the top to the bottom of the PCM domain. It is due to the evolution of natural convective currents in the enclosure as a result of buoyancy effect.

Further Fig. 4 clearly depicts that PCM melting process is considerably higher in cases 3 and 5. Longer fins, better approachability and locations of the fins in the enclosure assisted to expedite the melting process in both the cases.

Fig. 4 Liquid fraction contours of different cases at different time intervals



4.2 Enhancement Ratio

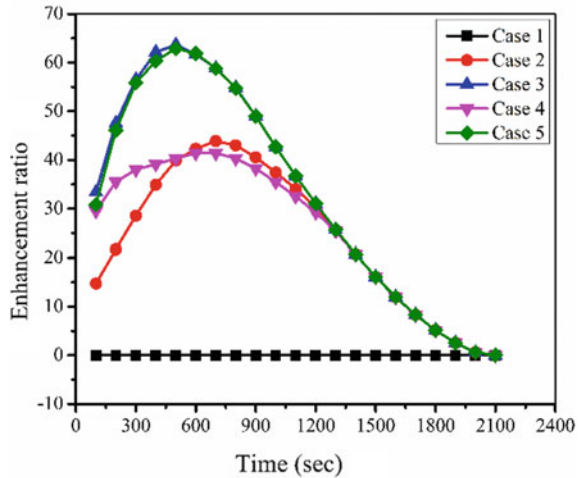
Enhancement Ratio (ER) is an indicator which shows the impact of fins inside the PCM enclosure. It provides the necessary information about liquid fraction of the PCM existing in the finned structure to the liquid fraction available in without fin configuration. Figure 5 illustrates the ER for all the cases with respect to time. It's noteworthy that case 1 is considered as reference PCM domain for the calculations of ER and assigned zero value of ER. Except case 1, all the cases have noticeable value of enhancement ratio which is being varied with time.

Figure 5 shows that value of ER for all the cases is increasing up to 500 s because by this time heat transfer mainly occurs through fins. Later on heat is transferred through PCM only. The highest value of ER is 63.6, 62.9, 43.8, 41.4 for the cases of 3, 5, 2 and 4, respectively. After certain period of time, all the curves are merged together because effect of fins has been diminished due to restriction of length.

4.3 Evolution of Stream Lines

To understand the characteristics of the streamlines formed during the melting process of the PCM, Fig. 6 has been drawn. It illustrates the streamlines in all the five cases evolved at time 400 s. Case 1 has only one vortex formation in the melted zone

Fig. 5 Enhancement ratio with respect to time for all the cases



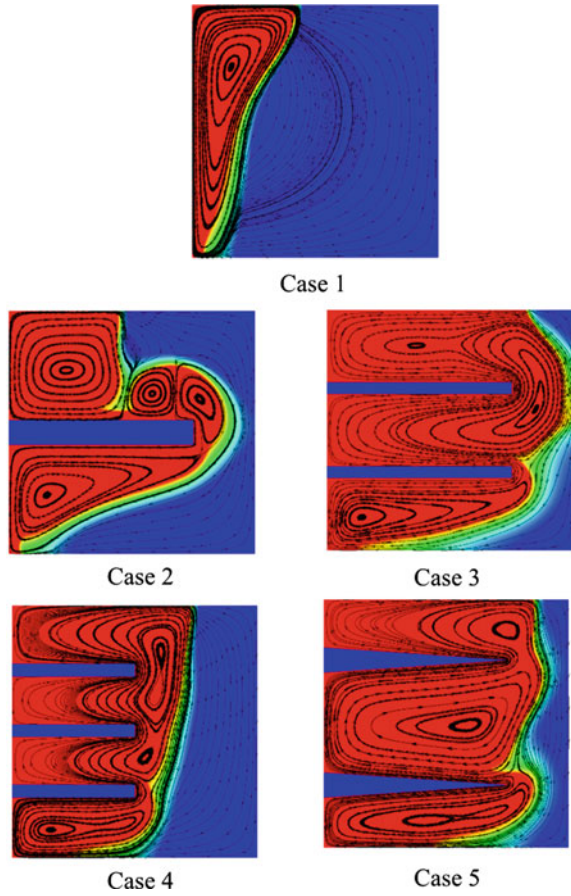
which continuously expands with time while in the finned enclosures, 3–4 eddies are formed. It is clearly visible that fins are mainly responsible for increasing the number of vortex formation. Figure 6 also shows that pattern of eddies is different based on number of fins and their geometries. Besides, vortices are more prominent close to the fins and there is no such pattern observed in the solid region of the PCM. It is worth mentioning that due to the formations of vortices, heat transfer via convective mode is significantly affected. It is clearly depicted that case 3 and 5 have a greater number of short and long loops of the streamlines due to which their melting rate is higher while, constrained length of the loops has been observed with case 4 due to which its melting rate is quite low as compared with other cases.

5 Conclusions

In the present study, two-dimensional transient numerical simulation has been performed for the square domain of PCM integrated with distinct fin configurations keeping equal heat transfer surface area of the fins. Impact of the various fin configurations is examined to understand the melting phenomenon of the PCM. Furthermore, evolution of the stream lines and enhancement ratio have also been obtained for each case. Following conclusion can be obtained from the present study.

- Fin arrangement, dimension and its location in the domain significantly affects the melting rate of the PCM.
- Cases 3 and 5 facilitate highest melting performance which is 60.4% higher than the case 1.
- Case 3 observes the maximum enhancement ratio whereas, least value is obtained with case 4.

Fig. 6 Streamline contours of the different cases at time interval of 400 s



- Owing to gravity, natural convective current generates in the enclosures, which is mainly responsible for the convective heat transfer.

Nomenclature

A	Area[m ²]
c_p	Heat capacity[J/kg-K]
ER	Enhancement ratio[-]
g	Gravity [m/s ²]
h	Enthalpy[kJ/kg]
k	Thermal conductivity[W/m-K]
T	Temperature [K]

t	Time[sec]
ρ	Density of air[kg/m ³]
β	Thermal expansion coefficient[-]
λ	Liquid fraction[-]

References

1. Mondal S (2008) Phase change materials for smart textiles—an overview. *Appl Therm Eng* 28(11–12):1536–1550
2. Rajabifar B (2015) Enhancement of the performance of double layered microchannel heatsink using PCM slurry and nanofluid coolants. *Int J Heat Mass Transf* 88:627–635
3. Khanna S, Reddy KS, Mallick TK (2018) Optimization of finned solar photovoltaic phase change material (finned pv pcm) system. *Int J Therm Sci* 130:313–322
4. Ji C, Qin Z, Low Z, Dubey S, Choo FH, Duan F (2018) Non-uniform heat transfer suppression to enhance PCM melting by angled fins. *Appl Therm Eng* 129:269–279
5. Chen SB et al (2021) Combined effect of using porous media and nano-particle on melting performance of PCM filled enclosure with triangular double fins. *Case Stud Therm Eng* 25:100939
6. Masoumpour-Samakoush M, Miansari M, Ajarostaghi SSM, Arıcı M (2021) Impact of innovative fin combination of triangular and rectangular fins on melting process of phase change material in a cavity. *J Energy Storage* 103545
7. Kamkari K, Shokouhmand H (2014) Experimental investigation of phase change material melting in rectangular enclosures with horizontal partial fins. *Int J Heat Mass Transf* 78:839–851
8. V. V. R. & P. C., “A Fixed grid numerical modelling methodology for convection diffusion mushy region phase change problems,” *Int. Journal Heat Mass Transf.*, vol. 30, no. 8, pp. 1709–1719, 1978.
9. Mat S, Al-Abidi AA, Sopian K, Sulaiman MY, Mohammad AT (2013) Enhance heat transfer for PCM melting in triplex tube with internal-external fins. *Energy Convers Manag* 74:223–236
10. Olfian H, Soheil S, Ajarostaghi M, Farhadi M (2020) Melting and solidification processes of phase change material in evacuated tube solar collector with u-shaped spirally corrugated tube. *Appl Therm Eng* 116149
11. Safari V, Abolghasemi H, Kamkari B (2021) Experimental and numerical investigations of thermal performance enhancement in a latent heat storage heat exchanger using bifurcated and straight fins. *Renew Energy* 174:102–121